Proceedings of the 21st ICSMGE, Vienna, Austria, 14 – 19 June 2026. Pistrol, Adam & Schweiger (eds.)
Published by: ÖGG, Austrian Society for Geomechanics, Salzburg, Austria, ISBN 978-3-9503898-4-5
https://doi.org/10.53243/ICSMGE2026-705

Application of machine learning algorithms for power output prediction in thermo-active diaphragm walls

Javier Sánchez Fernández,
Department of Civil and Environmental Engineering, Imperial College London, London, UK
Science and Solutions for a Changing Planet DTP, Grantham Institute, Imperial College London, London, UK

David M.G. Taborda
Department of Civil and Environmental Engineering, Imperial College London, London, UK

Agustín Ruiz López
Seequent – The Bentley Subsurface Company, Delft, The Netherlands

ABSTRACT: Thermo-active diaphragm walls offer an efficient route to low carbon heating and cooling by embedding heat-exchanging loops within deep retaining structures. In this study, a surrogate model to predict the power output per unit area of a diaphragm wall section is presented and evaluated. A parametrised 3D finite element (FE) model was created in COMSOL Multiphysics and used to assess 500 combinations of wall width and depth, concrete and soil conductivities, inlet–ground temperature differential, convective heat transfer coefficient at the exposed boundary, and fluid velocity. This was used as a numerical database for the training and testing of the surrogate model. The dataset covers 16 time instants retrieved from the transient analysis, in addition to the steady-state solution. The artificial neural network (ANN) regressor, subsequently trained, achieved an average coefficient of determination R^2 of 0.987. The average error in power prediction is limited to very few W/m^2, with the model being able to capture the correct trends even in the less accurate samples. Feature importance was carried out using SHAP analysis. This revealed that, as expected, the early time performance is dominated by the temperature differential and concrete conductivity, while the convective heat transfer coefficient at the exposed boundary governs long-term output. By replacing computationally expensive FE runs with fast ANN predictions, the proposed surrogate enables rapid design optimisation, sensitivity studies, and feasibility assessments for a large set of configurations.

KEYWORDS: Diaphragm wall, thermo-active structure, machine learning, energy geotechnics, finite element modelling.

1 INTRODUCTION

As global decarbonisation drives demand for electrified heating and cooling, thermo-active foundations have emerged as key enablers of net-zero buildings (Geological Society, 2022). By integrating heat-transfer circuits into diaphragm walls, structures can simultaneously serve as heat exchangers and retaining systems, improving the efficiency of urban land use (Amis et al., 2010). However, detailed finite element (FE) simulations of wall thermal performance remain computationally intensive, hindering rapid design evaluation. In this work, an artificial neural network (ANN) surrogate that learns from a comprehensive database generated using FE modelling is presented and its performance evaluated. The database is sampled via Latin hypercube across wall width and depth, concrete and soil thermal conductivities, fluid velocity, inlet-ground temperature differential, and convective heat transfer coefficient of the exposed boundary. The resulting model predicts power output per unit area at 16 time instants and at steady state with very fast inference times, retaining high fidelity with Mean Absolute Error (MAE) < 1.6 W/m² and steady state MAE = 0.8 W/m²). By coupling speed with interpretability using SHAP-based feature ranking, the methodology offers a practical decision platform for designing efficient, low-carbon diaphragm wall systems.

2 METHODOLOGY

2.1 *Finite Element modelling*

A 3D parameterised model of a thermo-active diaphragm wall was developed in COMSOL Multiphysics to generate the training dataset for the surrogate ANN. The computational domain comprised a 1.2 m wide section (i.e. in the out-of-plane direction) of the diaphragm wall, incorporating the optimised pipe layout detailed in Sterpi et al. (2020), embedded within soil extending about 30 m either side of the wall and L_{wall} + 20 m in the vertical direction, with boundary conditions as illustrated in Figure 1. The embedment depth was fixed to a constant value of 10 m. A single homogeneous soil layer was adopted, treating its thermal conductivity (k_{soil}) as a model parameter. The heat exchanger pipes, with internal diameter 26.2 mm and arranged as shown in Figure 2, were represented by linear elements capable of modelling both advective and diffusive heat transfer. Mesh generation via COMSOL's native mesher yielded an average of 200,000 quadratic elements per simulation. The meshing strategy consisted of generating very refined elements at the retaining wall to resolve steep thermal gradients, with elements progressively increasing in size towards the outer boundaries. Outlet fluid temperature was recorded at multiple time instants between 0 to 360 days. From these results, the instantaneous power output per unit wall area, P (W/m²), was determined using Equation (1), where ρ_w is the water density, c_w is the specific heat capacity of water, v_{fluid} is the fluid velocity, A_{pipe} is the pipe internal area, and T_{wall} is the wall thickness.

$$P = \frac{\rho_w c_w v_{fluid} A_{pipe} (T_{initial} - T_{inlet})}{T_{wall} \cdot 1.2\ m} \quad (1)$$

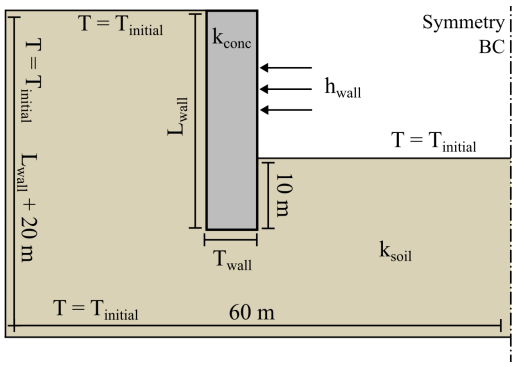

Figure 1. Schematic of the FE geometry and boundary conditions.

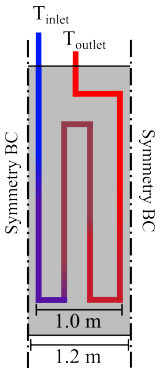

Figure 2. Pipe arrangement in the wall cross-section.

2.2 *Numerical data*

A total of 500 scenarios were created for the FE simulations using Latin Hypercube Sampling (LHS) (McKay et al., 1979), which provides a more uniform exploration of the input space than purely random approaches. The full range of geometric and material parameters is detailed in Table 1. These bounds are deliberately wide to capture different design conditions and thereby lead to a widely applicable surrogate. The resulting FE outputs then served as the database for training the ANN.

The convective heat transfer coefficient, h_{wall}, defined as the rate of heat exchanged per unit area per unit temperature difference, is a critical parameter for determining the performance of thermo-active walls (Bourne-Webb et al., 2016). In the presented model, it governs the convective boundary condition on the wall's exposed face, which is implemented via Newton's law of cooling shown in Equation (2), with $T_\infty = T_{initial}$. To cover an adequate spectrum of convective regimes, this coefficient was obtained by sampling via LHS over the range [-2,2], and then transforming the obtained value using the relation $h_{wall} = 2.5 \times 10^x$, which produced values ranging from ≈0 to 2500 $Wm^{-2}K^{-1}$, in line with expected field values (Theodore, 2011).

$$q = h_{wall}(T_s - T_\infty) \quad (2)$$

Table 1. FE model parameters.

Parameter	Symbol	Range	Unit
Total wall length	L_{wall}	20-60	m
Wall thickness	T_{wall}	0.8-1.2	m
Soil thermal conductivity	k_{soil}	0.5-3.0	$Wm^{-1}K^{-1}$
Concrete thermal conductivity	k_{conc}	1.0-3.0	$Wm^{-1}K^{-1}$
Heat transfer coefficient	h_{wall}	0-2500	$Wm^{-2}K^{-1}$
Initial temperature	$T_{initial}$	10-20	°C
Inlet temperature	T_{inlet}	0-8	°C
Pipe fluid velocity	v_{fluid}	0.1-1.0	m/s

2.3 *Artificial Neural Network*

An ANN regressor was constructed to predict the power output per unit area of the diaphragm wall, using 16 discrete time predictions to capture a year-long thermal performance plus a final steady-state value. The input feature set comprised the variables listed in Table 1, with the initial and inlet temperatures combined into a single temperature difference parameter $T_{diff} = T_{initial} - T_{inlet}$. The network was implemented in Keras (Chollet, 2021) and trained on an 80-10-10 split for training, validation, and testing datasets, respectively. Prior to training, all inputs and targets were standardised using StandardScaler.

The ANN architecture consisted of three fully connected hidden layers containing f=1000, 500, and 200 neurons, respectively, each followed by batch normalization, a ReLU activation, and a dropout layer (rate = 0.4). A final linear output layer produced the vector of predicted power values. A schematic representation of the architecture is provided in Figure 3. To optimise the ANN, a 10-fold GridSearchCV was used with the coefficient of determination R^2 as the performance metric, which identified an architecture of three hidden layers with 1 000, 500, and 200 neurons; a batch size of 20; a dropout rate of 0.4; and 400 training epochs. The initial learning rate was set to 0.001 and automatically reduced by 20% after 8 epochs without improvement. Training used mean squared error as the loss function and stopped after 25 epochs without improvement to prevent overfitting.

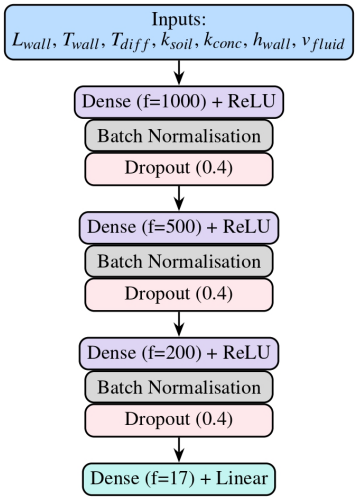

Figure 3. ANN architecture.

3 RESULTS

3.1 *FE data output*

The temperature results from the FE simulation confirm the expected results from the literature for similar wall configurations (Rammal et al., 2020). A typical thermal field is obtained, with temperatures extending outwards across the soil domain through heat conduction. Figure 4 shows four contours at different times for a sample with L_{wall} = 40 m.

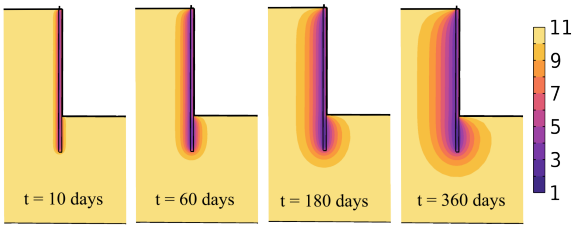

Figure 4. Temperature contours (°C) showing thermal fields after 10, 60, 180 and 360 days of operation.

3.2 *ANN model results*

The ANN surrogate demonstrates excellent accuracy in predicting the power output per unit area on the ground side face of the diaphragm wall under transient conditions. Table 2 reports the standard regression metrics, namely the Mean Absolute Error (MAE), Root-Mean-Square Error (RMSE), and coefficient of determination (R^2), at each of the 16 time points and final steady-state value. Across the full year, the MAE remains below 5.4 W/m², dropping to just 0.8 W/m² at steady state, while RMSE never exceeds 8 W/m² and settles at 1 W/m²

in the long term. R^2 values remain above 0.97 throughout, peaking at 0.994 around 2-5 days and only gently declining to 0.975 at steady state. The average R^2 over all time steps is approximately 0.986 which, compared to the 0.994 of the training dataset, confirms the model's robust generalisation and its ability to capture the different wall's thermal behaviour with high fidelity.

Table 2. Test dataset model accuracy metrics.

Time [day]	MAE [W/m^2]	RMSE [W/m^2]	R^2
0.01	5.4	7.9	0.982
0.05	3.5	5.1	0.987
0.10	2.9	4.3	0.988
0.25	2.2	3.3	0.990
0.50	1.7	2.6	0.991
0.75	1.5	2.2	0.992
1.0	1.4	1.9	0.993
2.0	1.0	1.3	0.994
5.0	0.7	0.9	0.994
10.0	0.7	0.8	0.992
20.0	0.7	0.9	0.988
30.0	0.7	0.9	0.986
60.0	0.8	1.0	0.981
90.0	0.8	1.0	0.980
180.0	0.8	1.0	0.977
360.0	0.8	1.0	0.976
Steady State (SS)	0.8	1.0	0.975

Figure 5 presents scatter plots of numerical versus ANN-predicted power output per unit area for the test set at four characteristic times: 1, 60, 180 and 360 days. The points cluster tightly around the 1:1 line, thus confirming the model accuracy across times and sample configurations.

Further analysis is shown in Figure 6, where the real and predicted results from three samples corresponding to the 25th, 50th and 75th percentiles in MAE are plotted. As shown, all samples are calculated with very high accuracy, with trends closely captured and minimal errors throughout.

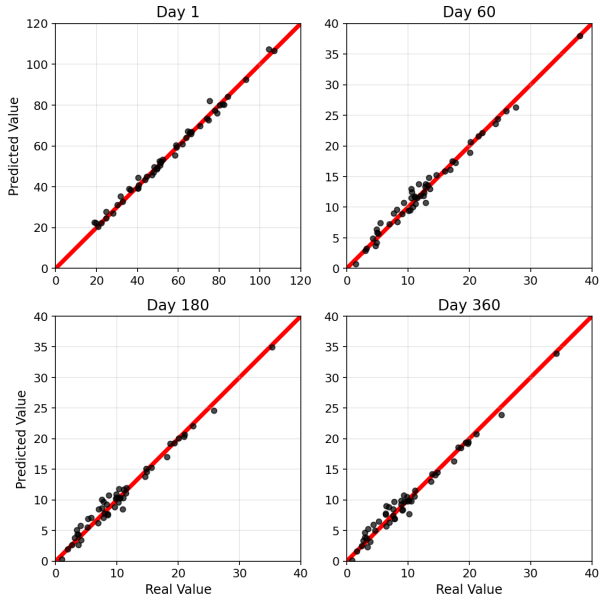

Figure 5. Real vs predicted model output at four different times.

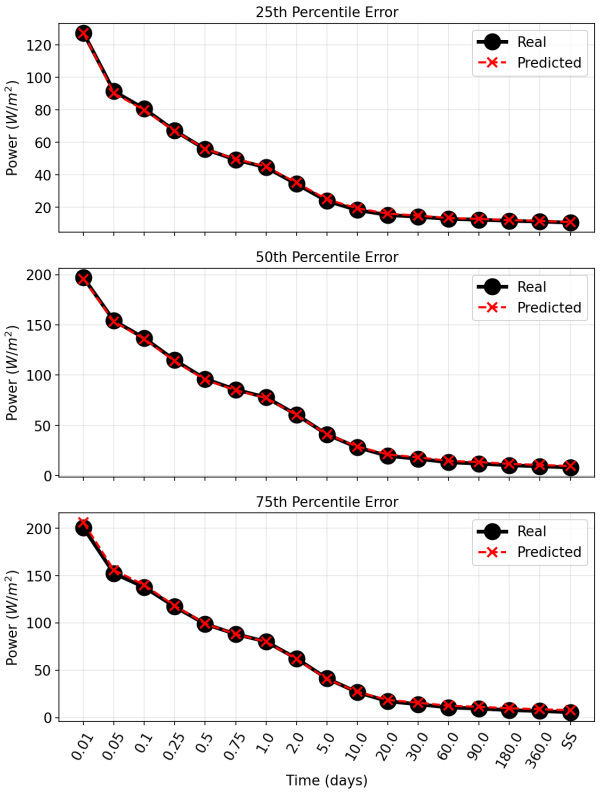

Figure 6. Real vs predicted power per unit area for samples at the 25th, 50th and 75th percentiles of the Mean Absolute Error (MAE).

3.3 *Feature importance*

An important aspect of any surrogate model is to provide interpretable results that justify decision making in the design. However, ANNs like the one presented in this work are known for acting as black boxes, unable to provide justification to their reasoning despite yielding very accurate predictions.

As a result of this, Lundberg & Lee (2017) provided a mathematically rigorous method to obtain feature importance referred to as SHapley Additive exPlanations (SHAP) values. This model-agnostic method quantifies the relative importance of each of the input features at obtaining the final output label, therefore enabling to rank these in terms of the overall contribution.

Figure 7 shows the average absolute SHAP value contributions for the seven inputs used in the surrogate model, averaged across all time values. Because a greater number of time instants are sampled during the earlier stages of the analysis, features that dominate short-term behaviour appear amplified in this aggregate view. For this reason, the temperature difference is the single most important factor at determining the power output of the wall, with the fluid velocity showing a non-negligible contribution.

If the steady state is considered in isolation, a different ranking is obtained, as shown in Figure 8. The most important input for determining the power output then becomes that governing heat transfer on the exposed side: knowing the boundary conditions at this side of the wall is essential to predict its output. This is in agreement with the results from Sailer et al. (2021). The difference between inlet and initial temperatures, together with the thermal conductivities of concrete and soil are the other significant contributing factors. On the other hand, the wall thickness, length and fluid velocity are less important for predicting the steady-state performance of thermo-active diaphragm walls. The value of h_{wall} at which the input produces no change in the output (zero SHAP value)

corresponds to 2.1 $Wm^{-2}K^{-1}$, which is close to the threshold of 2.5 $Wm^{-2}K^{-1}$ proposed by Sailer (2020) to distinguish between a fully insulated wall and a wall maintained at a constant temperature.

Figure 9 shows similar data, plotted in the form of a beeswarm plot, a common type of plot used to simultaneously depict each feature's impact magnitude and direction across all samples. The results agree with what is expected: greater convective heat transfer coefficients, temperature differences, thermal conductivities, and fluid velocity tend to increase the predicted power outputs, while greater wall dimensions decrease this quantity. Note that the latter is only true due to the power being normalised by the area of the wall, which reduces the importance of this aspect of the wall geometry, and given that boundary effects have a greater proportional impact on smaller walls.

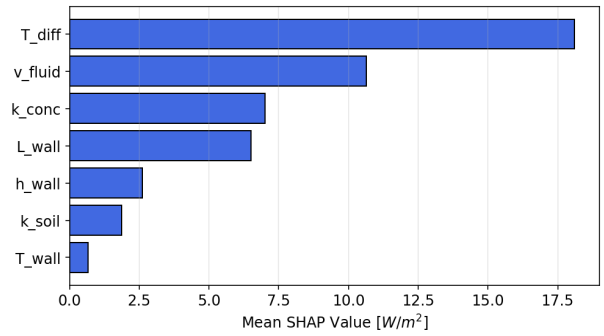

Figure 7. Mean SHAP value contributions.

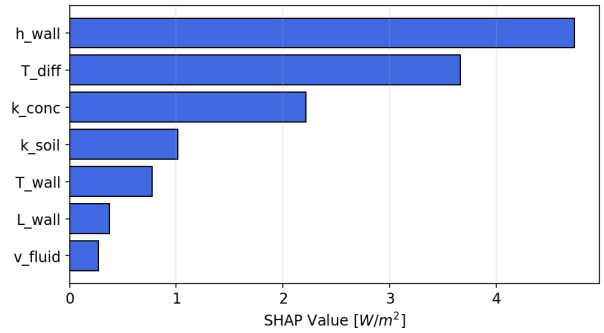

Figure 8. Steady-state SHAP value contributions.

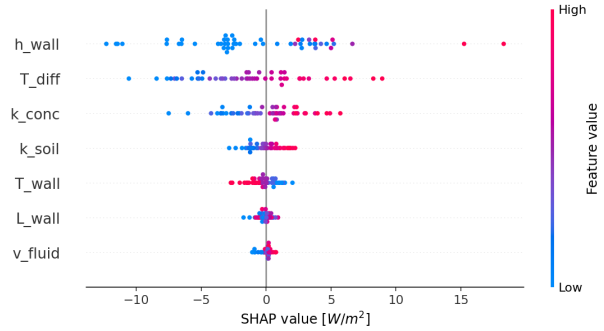

Figure 9. Beeswarm plot of steady-state SHAP values.

4 CONCLUSIONS

The presented study has demonstrated the viability and utility of a high-fidelity surrogate model for predicting the thermal performance of thermo-active diaphragm walls. By coupling a parametrised 3D FE model with an ANN trained on LHS simulations, the following can be concluded:

- The surrogate model can substitute computationally expensive FE simulations, predicting power output per unit area at 16 transient time steps plus the steady state with an average MAE below 1.6 W/m² (dropping to 0.8 W/m² at steady state).
- The model is accurate across all time outputs, with particularly high accuracy during the initial times, achieving an average R^2 test set score of 0.986.
- SHAP-based feature importance analysis shows that the temperature difference and concrete thermal conductivity govern early time behaviour, whereas the exposed face boundary condition dominates at longer times.

The work presented aims to demonstrate the potential of surrogate models at predicting the thermal performance of a wide range of thermo-active wall configurations. The accurate results, combined with the significantly faster computational speeds compared to conventional calculations or FE simulations make this surrogate a great starting point for engineers and designers evaluating low-carbon foundation solutions.

5 ACKNOWLEDGEMENTS

This research is part of the SaFEGround (Sustainable, Flexible and Efficient Ground-source heating and cooling systems) project, which is funded by the Engineering and Physical Sciences Research Council (EPSRC) (grant number: EP/V042149/1), and part of the SIDeTools (Sustainable Infrastructure Design Tools) project, funded by the Engineering and Physical Sciences Research Council (EPSRC) (grant number: EP/X52556X/1). This work was also supported by the Natural Environment Research Council [NE/S007415/1].

6 REFERENCES

Amis, T., Robinson, C.A.W., Wong, S., 2010. Integrating Geothermal Loops into the Diaphragm Walls of the Knightsbridge Palace Hotel Project. Proceeding of the 11th DFI / EFFC International conference, London 10.

Bourne-Webb, P.J., Bodas Freitas, T.M., Da Costa Gonçalves, R.A., 2016. Thermal and mechanical aspects of the response of embedded retaining walls used as shallow geothermal heat exchangers. Energy Build 125, 130–141.

Chollet, F., 2021. Deep Learning with Python. Manning Publications, New York, United States.

Geological Society, 2022. Decarbonising heat with geothermal energy. Available at: https://www.geolsoc.org.uk/science-and-policy/policy/briefing-notes-and-position-statements/decarbonising-heat-geothermal-energy/ [Accessed 23rd July 2025].

Lundberg, S.M., Lee, S.I., 2017. A unified approach to interpreting model predictions. Advances in Neural Information Processing Systems, Issue 2, 4766–4775.

McKay, M.D., Beckman, R.J., Conover, W.J., 1979. A comparison of three methods for selecting values of input variables in the analysis of output from a computer code. Technometrics 42, 55–61.

Rammal, D., Mroueh, H., Burlon, S., 2020. Thermal behaviour of geothermal diaphragm walls: Evaluation of exchanged thermal power. Renewable Energy 147, 2643–2653.

Sailer, E., 2020. Numerical Modelling of thermo-active retaining walls (PhD Thesis). Imperial College London.

Sailer, E., Taborda, D.M.G., Zdravković, L. and Potts, D.M., 2021. A novel method for designing thermo-active retaining walls using two-dimensional analyses. *Proceedings of the Institution of Civil Engineers - Geotechnical Engineering*, 175(3), 289–310.

Sterpi, D., Tomaselli, G., Angelotti, A., 2020. Energy performance of ground heat exchangers embedded in diaphragm walls: Field observations and optimization by numerical modelling. Renew Energy 147, 2748–2760.

Theodore, L., 2011. Heat Transfer Applications for the Practicing Engineer. Hoboken, NJ: John Wiley & Sons, Inc.